

Vigneshkumar Alagarsamy<sup>1\*</sup>, Clementz Edwardraj Freeda Christy<sup>1</sup>, Muthukannan Muthiah<sup>2</sup>, Ubagaram Johnson Alengaram<sup>3</sup>

<sup>1</sup>Department of Civil Engineering, Kalasalingam Academy of Research and Education, Krishnankoil, Tamil Nadu, India, <sup>2</sup>Department of Civil Engineering, KGC College of Technology, Karapakkam, Chennai, Tamil Nadu, India, <sup>3</sup>Centre for Innovative Construction Technology (CICT), Department of Civil Engineering, Faculty of Engineering, Universiti Malaya, Kuala Lumpur, Malaysia.

Scientific paper

ISSN 0351-9465, E-ISSN 2466-2585

<https://doi.org/10.62638/ZasMat1181>



Zastita Materijala 66 (2)  
280 - 291 (2025)

## Influence of alkaline binders on the workability and strength of self compacting geopolymer concrete

### ABSTRACT

*Selfcompacting geopolymer concrete (SCGC) is a promising alternative to traditional concrete due to its environmental benefits. In SCGC, alkaline binders such as sodium hydroxide (NaOH) and sodium silicate ( $\text{Na}_2\text{SiO}_3$ ) have the potential to influence both workability and strength. Particularly, the ratio of alkaline binders impacts directly the overall performance of SCGC. In this research, five SCGC mixes with various alkaline binder ratios between 0.40 to 0.60 in 50% fly ash (FA) and 50% ground granulated blast furnace slag (GGBS), at a concentration of 14 M NaOH, superplasticizer ( $9\text{kg/m}^3$ ) and extra water ( $54\text{kg/m}^3$ ) were investigated for the effect of alkaline binder ratio on workability and mechanical strength properties. The study results showed that the fresh properties of SCGC with A/B ratios of 0.4, 0.45 and 0.5 complied with EFNARC guidelines from the slump flow test and the lowest  $T_{50\text{cm}}$  slump obtained was 696 mm. The highest CS of 38.3 MPa, STS of 4.63 MPa, and FS of 5.85 MPa have been attained, which indicated better mechanical performance of the SCGC mix with a 0.5 A/B ratio. Therefore, the 0.5 alkaline binder ratios were optimized at 14M of NaOH on rheological and strength properties.*

**Keywords:** Fly ash, GGBS, NaOH,  $\text{Na}_2\text{SiO}_3$ , Alkaline binder ratio, Rheological and mechanical properties.

### 1. INTRODUCTION

The world is focusing on sustainable and high-performance building technology to minimize the significance of construction on the environment and human health, which has low harmful emissions [1]. Geopolymer concrete (GPC) is a greener option because it reduces dependence on Portland cement production [2]. In addition, GPC offers a more sustainable and potentially higher performing alternative to conventional concrete [3].

The traditional concrete process generates significant carbon emissions [4]. The GPC utilizes fly ash (FA) and ground granulated blast furnace slag (GGBS) and is widely recognized as valuable supplementary cementitious materials (SCMs) in the construction industry due to their pozzolanic and

hydraulic properties, respectively [5,6]. At the same time, GPC can achieve higher compressive (CS) and tensile strengths (STS) than traditional concrete. It also exhibits lower shrinkage and cracking, leading to durable structures [7]. However, high viscosity nature of GPC makes it prone to inadequate compaction [8]. The self-compacting geopolymer concrete (SCGC) was introduced to resolve this issue [9]. SCGC is a pourable concrete mix that achieves compaction under its weight, eliminating the need for mechanical vibration during placement, which can flow readily, filling complex shapes and congested reinforcement areas without vibration [10,11]. Nevertheless, the concentration of the alkali activator solution affects both fresh and hardened properties [12]. Furthermore, a higher molarity of alkali activator can enhance strength but may decrease workability due to a faster setting [13].

Generally, FA contributes to better workability in SCGC due to its finer particle size and spherical shape, which improve particle packing and lubrication within the mix, allowing for smoother flow [14,15]. Regardless, GGBS reacts more

\*Corresponding author: Vigneshkumar Alagarsamy

E-mail: [eng.vigneshkumar@gmail.com](mailto:eng.vigneshkumar@gmail.com)

Paper received: 18. 07. 2024.

Paper corrected: 28. 09. 2024.

Paper accepted: 02. 10. 2024.

rapidly with the alkaline activator when compared to FA, which translates to faster setting times and higher early strength development, making it beneficial for precast applications [16,17]. Furthermore, the volume fraction and size distribution of coarse aggregates affect the packing density and workability of SCGC [18,19]. For instance, proper grade aggregates with a suitable particle size can help to aid the packing of particles within the concrete matrix, which improves its mechanical properties and workability [20,21]. Typically, angular and irregularly shaped aggregates with rough surfaces provide better interlocking and resistance to segregation compared to rounded aggregates [22]. At the same time, the particle size and shape of fine aggregates also influence the rheology and flow characteristics of SCGC [23]. Commonly, the finer particles improve the packing density and fill voids between coarse aggregates, enhancing the homogeneity and workability of the mix [24]. Fine aggregates contribute to the overall surface area available for geopolymerization reactions. In addition, superplasticizer (SP) are high-range water reducers that disperse cementitious particles more effectively, reducing the water to binder ratio without sacrificing workability [25]. In SCGC, where geopolymer binders are used instead of Portland cement, SP helps in achieving the desired flow ability and filling ability necessary for self-compaction [26,27]. The use of superplasticizer in SCGC can lead to reduced water and cementitious material content, resulting in economic savings and environmental benefits [28].

The alkaline binder ratio (A/B ratio) has the potential to influence directly and initiate the progression of the geopolymerization reaction, including forming the three-dimensional network of aluminosilicate gel that binds the concrete together [29,30]. Additionally, it can accelerate the geopolymerization process, leading to faster setting times and early strength development in higher ratios [31]. It largely affects the rheological properties of SCGC, including workability, flow ability, and viscosity [32]. In contrast, sodium silicate ( $\text{Na}_2\text{SiO}_3$ ) can sometimes lead to delayed setting times in SCGC mixes, especially in high concentrations and improper optimization of the A/B ratio [33]. On the other hand, excessive amounts of  $\text{Na}_2\text{SiO}_3$  can decrease the workability of SCGC mixes, which are difficult to place and compact [34]. According to the study, adjusting the A/B ratio can facilitate a more fluid mix, which improves workability and aids the self-compaction nature of GPC [35]. Therefore, it must ensure that SCGC can flow to fill intricate formwork and densely reinforced areas without the external need for vibration by optimizing the A/B [36]. At the same time, the A/B

ratio has a significant role in controlling the early-age and long-term strength of SCGC [37]. For instance, the higher activator concentrations promote faster strength gain due to accelerated geopolymerization kinetics [38]. However, excess high activator ratios may lead to rapid stiffening and premature strength development, which leads to workability compromise in the long term [39].

On the other hand,  $\text{Na}_2\text{SiO}_3$  production is a highly energy-intensive process, which has high carbon footprints for GPC [40]. In  $\text{Na}_2\text{SiO}_3$  production, soda ash and silica sand are mixed and heated in a furnace at temperatures above  $1300^\circ\text{C}$ , which forms  $\text{Na}_2\text{SiO}_3$  along with carbon dioxide gas [41]. Accordingly, optimizing the A/B ratio may require a lower amount of  $\text{Na}_2\text{SiO}_3$ , which can help to decrease carbon footprints and support environmental protection [42]. This research explores the effect of different alkaline binder ratios of 0.40 to 0.60 with an interval of 0.05 on rheological and mechanical behavior of FA (50%) and GGBS (50%) based SCGC, and the ratio of  $\text{Na}_2\text{SiO}_3$  to NaOH as 1:2.5 at a concentration of 14 M NaOH, superplasticizer ( $9\text{kg/m}^3$ ) and extra water ( $54\text{kg/m}^3$ ) and then tests were conducted including slump flow test,  $T_{50\text{cm}}$  slump flow test, V-funnel and L-box to assess the rheological properties of SCGC. The Compressive Strength (CS), Split Tensile Strength (STS) and Flexural Strength (FS) of SCGC were examined at 7 and 28 days. Also, this study provides suggestions and recommendations for A/B ratio optimization.

## 2. MATERIALS AND METHODS

### 2.1. Fly ash and GGBS

An FA (class F) was acquired from the Tamil Nadu Coal-fired Thoothukudi power plant and used for this study. The specific gravity of the FA is 2.1. GGBS is a feedstock material used in SCGC that comes from the massive amounts of solid waste produced as a product of the iron and steel industries [43]. The specific gravity of GGBS acquired from the JSW (Jindal Steel Works) plant in Madurai, was 2.9. FA and GGBS morphology was examined using a Scanning Electron Microscope (SEM) ZEISS EVO 18, manufactured by ZEISS (Japan). The SEM was fitted along with EDX (EDAX APEX systems) and was used to analyze the microstructure of SCGC. The minerals and crystalline structure present in FA and GGBS were analyzed using an X-ray diffractometer (BRUKER D8 model), with XRD patterns recorded in the  $2\theta$  range of  $10^\circ$  to  $80^\circ$ . Using Bruker S8 Tiger (Germany) XRF spectroscopy, a qualitative and quantitative analysis of the material composition was carried out.

## 2.2. Alkaline activator

The alkaline solution is essential to the geopolymerization process because it initiates the reaction between aluminosilicate minerals that forms the geopolymer structure. An alkaline mixture containing solutions of sodium hydroxide (NaOH) and sodium silicate ( $\text{Na}_2\text{SiO}_3$ ) in 1:2.5 ratio was used in this study. With the specific gravities of 1.47 and 1.6 respectively, these solutions were thoroughly mixed and agitated for 24 hours before casting the specimen.

## 2.3. Aggregates

In this study, 12.5 mm sizes coarse aggregate (CA) and fineness modulus of 7.16 with 2.83 of specific gravity were adopted. Manufacture sand (M-sand) the by-product of crushing from quarries as fine aggregate with 2.65 of fineness modulus and 2.73 of specific gravity was utilized.

## 2.4. Superplasticizer

Superplasticizer plays a vital role in achieving the desired workability. MasterGlenium Sky 8233 is a new generation superplasticizer based on modified polycarboxylic ether purchased from Astra Chemicals, Chennai. It has density of  $1080 \text{ kg/m}^3$ , which was used to improve the process ability and flow.

## 2.5. Mix Proportion

The SCGC mixes were completed in accordance with the EFNARC SCC criteria. The mix proportion of SCGC is tabulated in Table 1. The mix designations with a total binder content of  $450 \text{ kg/m}^3$  as 50% of FA and 50% of GGBS. The ratio of sodium silicate to sodium hydroxide was 1:2.5 at a concentration of 14 M sodium hydroxide. The alkali solution to binder was 0.40 to 0.60 and 2% ( $9 \text{ kg/m}^3$ ) superplasticizer and 12% ( $54 \text{ kg/m}^3$ ) extra water was used in this research.

Table 1. Mix the proportion of SCGC

Mix ID	A/B ratio	FA $\text{kg/m}^3$	GGBS $\text{kg/m}^3$	Fine aggregate $\text{kg/m}^3$	Coarse aggregate $\text{kg/m}^3$	NaOH $\text{kg/m}^3$	$\text{Na}_2\text{SiO}_3$ $\text{kg/m}^3$	Molarity	SP ( $\text{kg/m}^3$ )	Extra water ( $\text{kg/m}^3$ )
S1	0.40	225	225	961.08	786.33	53.27	133.75	14	9	54
S2	0.45	225	225	961.08	786.33	57.86	144.66	14	9	54
S3	0.50	225	225	961.08	786.33	62.14	155.37	14	9	54
S4	0.55	225	225	961.08	786.33	66.15	165.39	14	9	54
S5	0.60	225	225	961.08	786.33	69.91	174.79	14	9	54

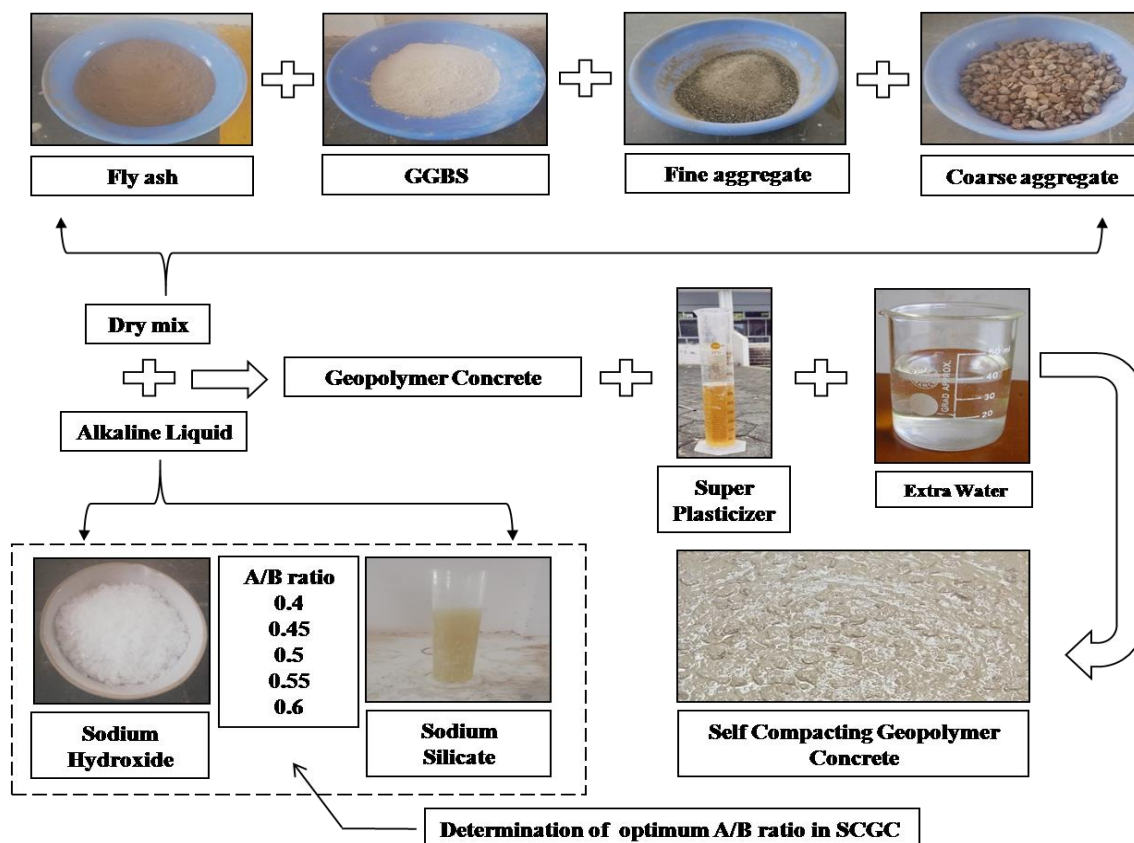


Figure 1. SCGC production process

## 2.6. Blending, casting, processing, and curing

FA, GGBS and aggregates in a saturated, surface-dry state were mixed in 100-litre pan mixers for about 2.5 minutes. This dry mixing process ensures an even distribution of aggregate, FA and GGBS. After dry mixing, a liquid mixture of an alkaline solution, SP and additional water were added to the mix. Wet mixing was continued for 3 minutes and ensures thorough incorporation of the liquid mixture into the dry components. Finally, the specimens were removed from the molds and the SCGC specimens were cured at room temperature until they were ready for testing at all stages of cure. The SCGC manufacturing process is shown in Figure 1.

## 3. EXPERIMENTAL PROGRAMS

### 3.1. Rheological properties of SCGC

Slump flow,  $T_{50\text{cm}}$  slump flow, L-box, and V-funnels tests were conducted on the SCGC mixture. The slump flow test estimates the flowability of the SCGC mix by observing the spreading diameter of the concrete when it slumps after demolding from conical molds. It provides

information on the workability and filling capacity of the concrete mix. The 50 cm flow test measures the time it takes for the mix to spread a diameter of 50 cm after it has been removed from a mold, thereby assessing the quantitative filling and flow ability of the concrete [44]. Testing with L-boxes was performed to determine the concrete's resistance to reinforcement. L-box tests consider the flow heights of the concrete based on the vertical section ( $H_1$ ) and the horizontal component ( $H_2$ ). The V-funnel test evaluates the flowability and consistency of the concrete by measuring the flow with a funnel from a standardized opening. It provides information on the flow properties and workability of the fresh self compacting concrete mix.

### 3.2. Mechanical properties of SCGC

The analysis of SCGC based on FA and GGBS for compressive, split tensile, and flexural at various curing periods of all ages was carried out. For the CS test, cube specimens of 100 mm x 100 mm x 100 mm (Figure. 2a) and cylindrical specimens with 100 mm diameter and 200 mm height were cast for the STS test (Figure. 2b).

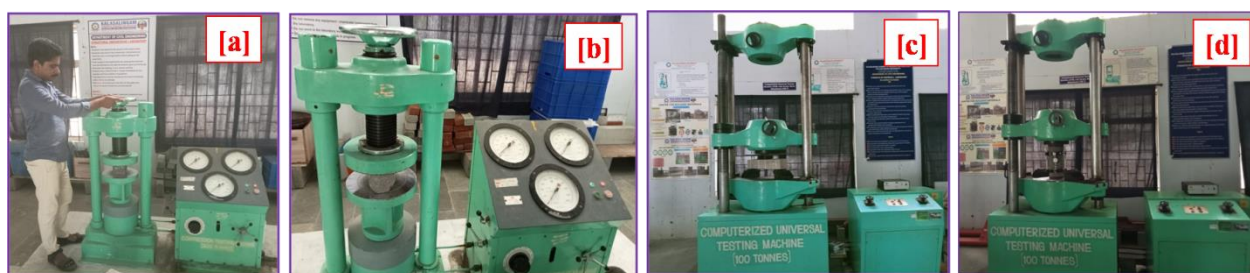


Figure 2. (a, b, c and d) examination of SCGC's mechanical characteristics

Prismatic specimens measuring 100 mm x 100 mm x 500 mm were cast for the FS test. Cube-shaped specimens were tested using a Compression Testing Machine (CTM) according to the IS: 516-1959 after 7 and 28 days for CS [45]. The STS tests were carried out for all ages according to the IS: 5816-1999 [46]. FS of SCGC, prism-shaped specimens were tested using a Universal Testing Machine (UTM) with a capacity of 400 kN after 7 and 28 days as per IS: 516-1959 to determine the FS shown in (Figure. 2 c) [45]. The modulus of elasticity of SCGC was carried out in accordance with IS: 516-1959 on cylindrical specimens with a diameter of 150 mm and a height of 300 mm at the age of 28 days for the ratio of stress to strain under the action of loads. An extensometer with a dial gauge was placed at the centre of the cylindrical specimen to measure the deformation of the SCGC cylindrical specimen. The specimens were compressed under the action of a unidirectional compressive load, shown in Figure

2d, and loaded at a displacement rate of 1.4 to 1.6 kg/minute.

## 4. RESULTS AND DISCUSSION

### 4.1. Characterization of FA and GGBS

The FA and GGBS were characterized to utilize of SCGC's precursors. From Figure 3. (A&B), the SEM demonstrates that the FA particles are smooth-surfaced as well as spherical in shape. The rough surfaces and irregular shapes of GGBS are depicted in Fig. 3 (C&D). X-ray diffraction was used to analyze the elements of FA and GGBS, as seen in Figs. 4 and 5. Figure 4. displays the elements present in FA derived from an EDAX spectrum. The principal ingredients are aluminium (15.3%) and silicon dioxide (22.3%). The minor components of FA are potassium (1.2%), magnesium (1.2%), and iron (3.7%). According to GGBS's elemental study (Figure 5), silicon dioxide (12%) and calcium (22.5%) formulate the majority of the material. In GGBS, magnesium (4.3%) and aluminum (7.4%) are the two most significant constituents.



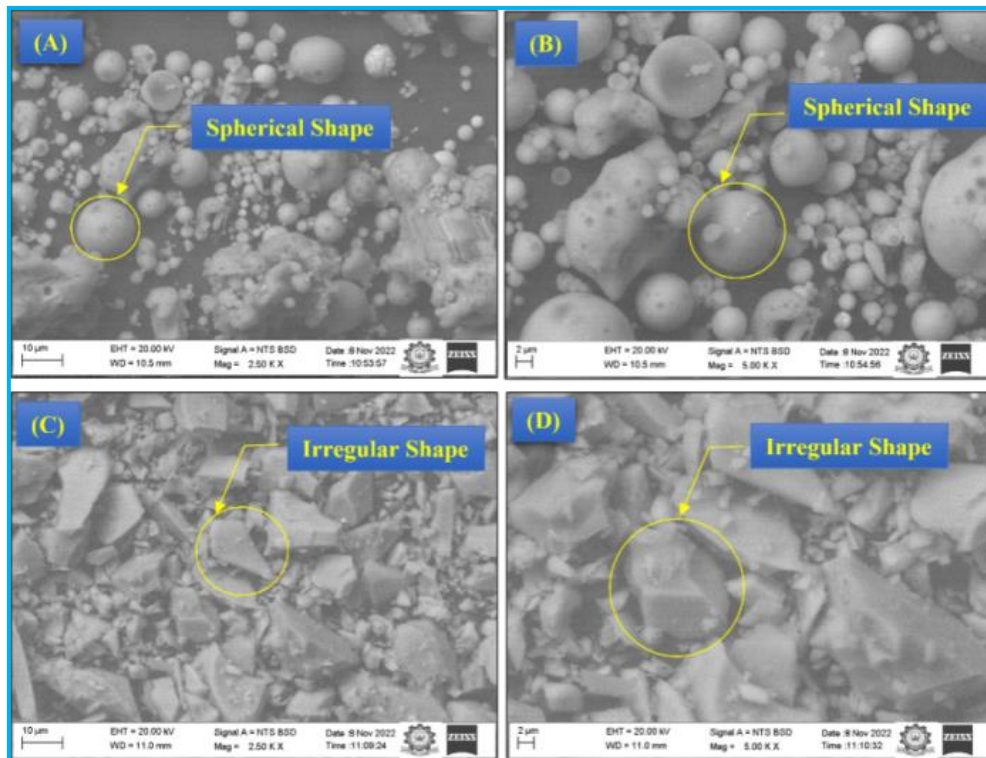


Figure 3. FA (A&B), GGBS (C&D) scanning electron micrograph

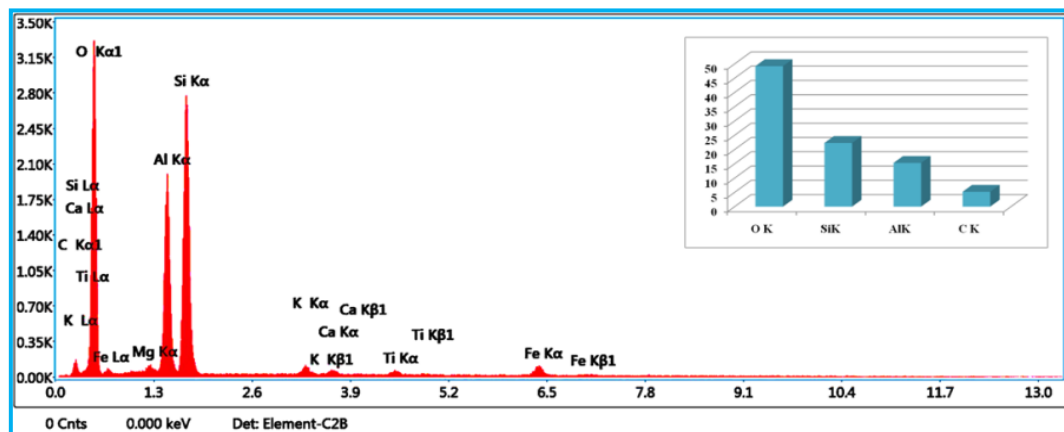


Figure 4. Elemental study of FA with Energy-Dispersive X-rays

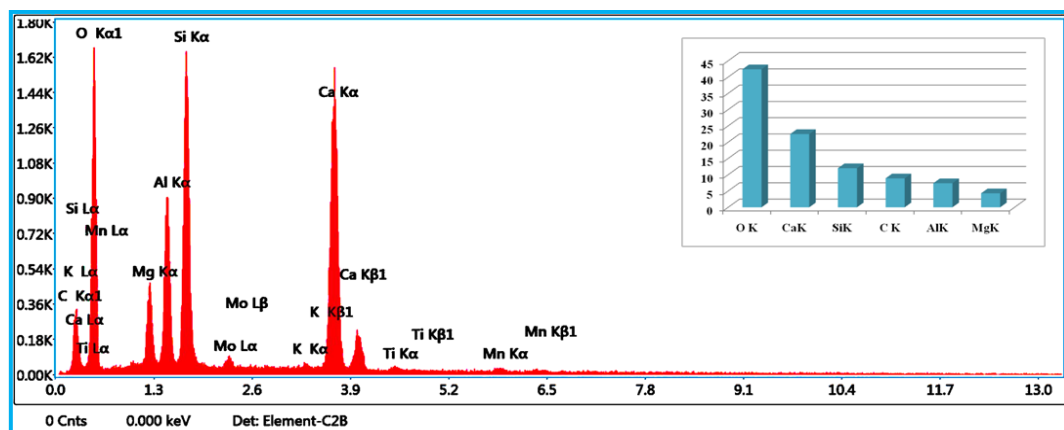


Figure 5. Elemental study of GGBS with Energy-Dispersive X-ray

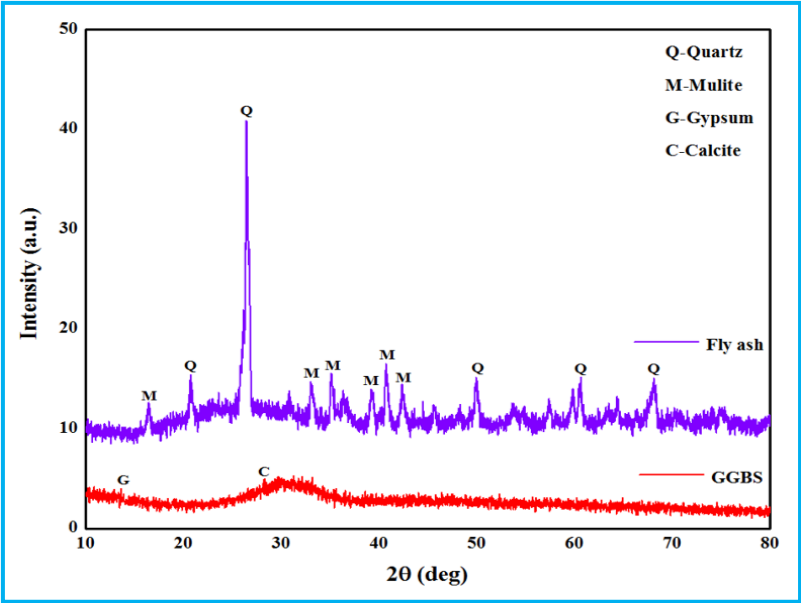


Figure 6. FA and GGBSXRD patterns

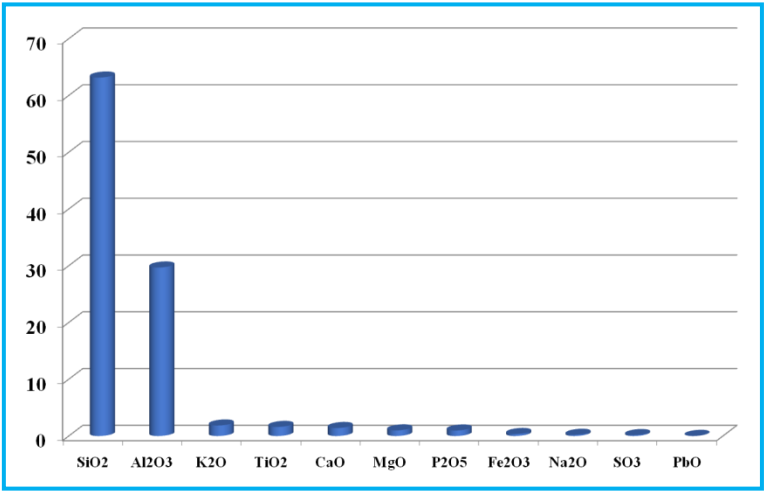


Figure 7. Chemical Composition of FA

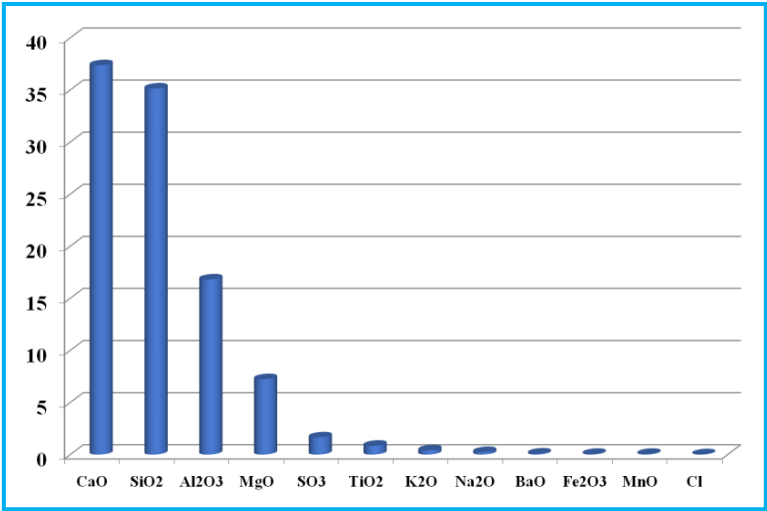


Figure 8. Chemical composition of GGBS

The purity of FA was obtained with X-ray diffraction (XRD) Quartz (silicon dioxide,  $\text{SiO}_2$ ) and mullite (aluminium oxide,  $\text{Al}_2\text{O}_3$ ) are its two primary crystalline phases. GGBS, as illustrated in Figure 6, has an amorphous phase of calcite ( $\text{CaCO}_3$ ) and a semi-crystalline structure of gypsum ( $\text{CaSO}_4$ ).

Figures. 7 and 8 illustrate the chemical composition of GGBS and FA. From XRF findings, 63.16% of  $\text{SiO}_2$  and 29.69% of  $\text{Al}_2\text{O}_3$  were found predominantly in the FA the XRF result indicates that the main concentrations of 37.37% of CaO, 35.14% of  $\text{SiO}_2$ , 16.81% of  $\text{Al}_2\text{O}_3$  and 7.24% MgO were predominantly found in the GGBS.

#### 4.2. Rheological properties of SCGC

The rheological properties, which describe the flow behavior and workability of SCGC, are often assessed using several standard tests. These tests include the slump flow test,  $T_{50\text{cm}}$  slump flow test, V-funnel test, and L-box test. Table 2. *Rheological characteristics of SCGC mix.*

Table 2. *Rheological characteristics of SCGC mix*

Mix ID	Slump flow (mm)	$T_{50\text{cm}}$ flow (Sec)	V –funnel (Sec)	L-BOX
S1	762	2.6	7.4	0.95
S2	733	3.4	8.5	0.91
S3	696	4.3	9.8	0.86
S4	642	5.9	12.5	0.79
S5	617	7.8	14.4	0.77

##### 4.2.1. Slump flow test

The slump flow test is carried out to assess the workableness and processability of SCGC. It measures the flow spread diameter of the concrete mixture when it slumps after being released from a conical mold. The results are shown in Table 2 and Figure 9.

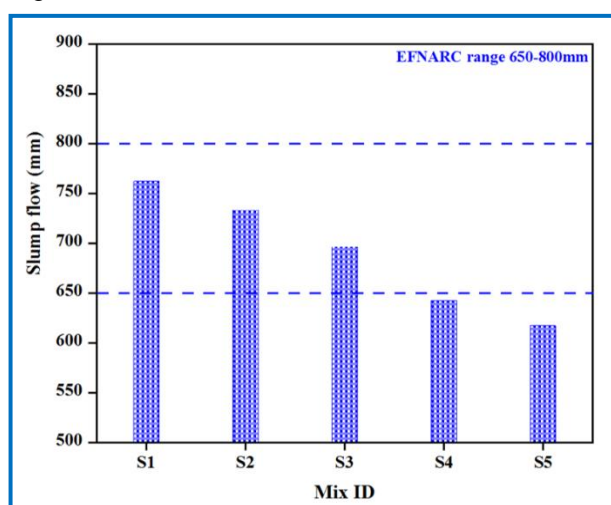


Figure 9. *Slump flow test*

It shows that all blends are within the EFNARC range of 650 mm to 800 mm. Slump flow from

alkaline binder Mix ID - S1 to S5 was attained as 762mm, 733mm, 696mm, 642 mm, and 617mm respectively. The maximum flow has achieved as 762mm at Mix ID - S1 and minimum flow was received as 617mm for Mix ID -S5.

It was found that the slump flow of the SCGC mixtures decreases with increasing alkaline binder content.

##### 4.2.2. $T_{50\text{cm}}$ flow test

The time it takes for the concrete to spread at a diameter of 50 cm is analyzed utilizing the Slump- $T_{50\text{cm}}$  test as shown in Table 2 and Figure 10. It can be seen that except for Mix ID S4 and S5 and five SCGC mixes, the allowable limits specified by EFNARC (2-5 sec) were achieved. It varies between 2.6 and 7.8 and the lowest value of 2.6 sec is reached for Mix ID -S1.  $T_{50\text{cm}}$  time from Mix ID- S1 to S5 has received 2.6, 3.4, 4.3, 5.9 and 7.8 respectively. It can be observed that increasing the alkaline binder content increases the  $T_{50\text{cm}}$  time.

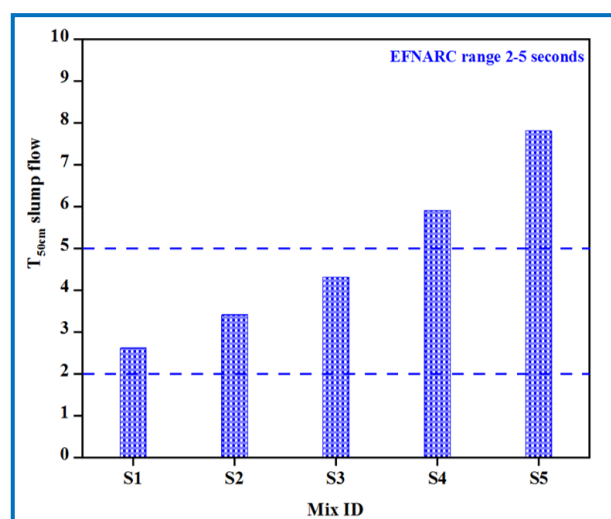


Figure 10.  *$T_{50\text{cm}}$  flow test*

##### 4.2.3. V-funnel flow time

The V-funnel test serves as a crucial method for evaluating the flowability and workability of SCGC mixtures. This test assesses the time it takes for the concrete to flow through a V- funnel, providing insights into its rheological properties and suitability for various construction applications. The observed values are shown in Table 2 and Figure 11

The flow time is between 7.4 and 14.4 sec. All three SCGCs met the acceptable flow time other than Mix ID - S4 and S5. The v-funnel flow time from Mix ID - S1 to S5 has received 7.4, 8.5, 9.8, 12.5, and 14.4 sec respectively.

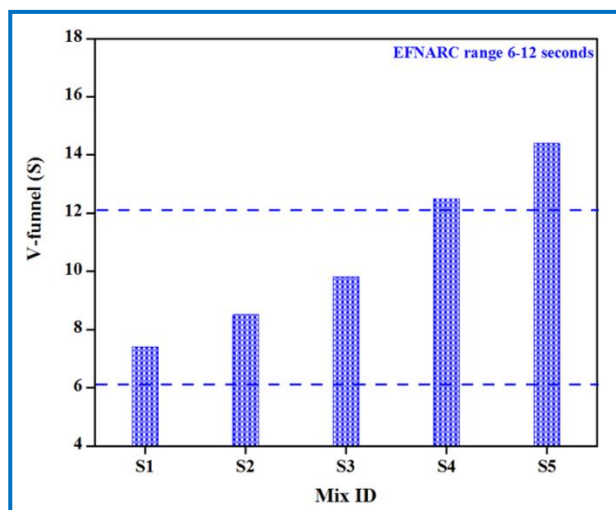


Figure 11. V-funnel test

#### 4.2.4.L-box test

The L-box test is one of the most common and effective methods for determining the passing ability of SCC. The blocking ratio ( $H_2/H_1$ ) of SCGC is shown in Table 2 and Figure 12. According to EFNARC, the permissible range for SCGC is between 0.8 and 1.0.

The observation shows that the  $H_2/H_1$  ratio decreases with increasing proportions of alkaline binders. It can be seen that with the exception of Table 3. Strength characteristics of SCGC mix

Mix ID - S4 and S5 and the other SCGCs, the allowable range for SCGC is below 0.8 to 1.0 compared to all other mixtures. This test height ratio of Mix ID - S1 to S5 has obtained 0.95, 0.91, 0.86, 0.79 and 0.77 respectively.

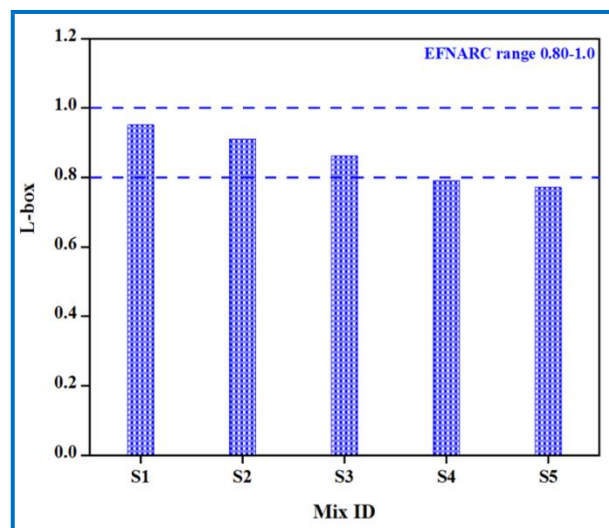


Figure 12. L-box test

#### 4.3. Hardened properties of SCGC

CS, STS, and FS are indeed crucial for evaluating the mechanical properties of SCGC. Table 3. Strength characteristics of SCGC mix.

Mix ID	Compressive strength (MPa)		Splitting tensile strength (MPa)		Flexural strength (MPa)		Modulus of elasticity (MPa)
	7 days	28 days	7 days	28 days	7 days	28 days	
S1	20.8	28.3	2.6	3.84	3.64	4.86	26599
S2	25.1	34.5	2.9	4.14	3.91	5.24	29368
S3	27.6	38.3	3.4	4.63	4.28	5.85	30943
S4	25.4	36.6	3.2	4.39	4.16	5.52	30249
S5	23.8	34.2	3.1	4.03	3.83	5.3	29240

##### 4.3.1.Compressive strength

CS is indeed a crucial characteristic evaluating the performance and quality of concrete. The CS for all five components after 7 and 28 days is shown in Table 3 and Figure 13. A maximum of 27.6 MPa and 38.3 MPa was observed for mix ID - S3 after 7 and 28 days. The 7-day CS for Mix ID - S2 to S5 developed a strength increase of 17.13 %, 24.63 %, 18.11 % and 12.60 % compared to the control sample of Mix ID -S1.

The 28-day CS for Mix ID -S2 to S5 developed a strength increase of 17.97 %, 26.10 %, 22.67 % and 17.25 % compared to the control sample Mix ID -S1. Overall, the CS of the SCGC improved by 12.78 %

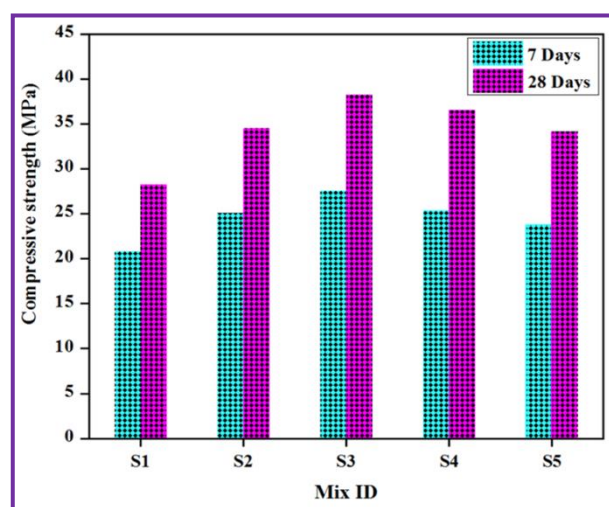


Figure 13. Compressive strength test



The 28-day CS for Mix ID -S2 to S5 developed a strength increase of 17.97 %, 26.10 %, 22.67 % and 17.25 % compared to the control sample Mix ID -S1. Overall, the CS of the SCGC improved by 12.78 %.

#### 4.3.2. Split tensile strength

The results of STS tests for SCGCs with different alkaline binder correspondences for all the five mixtures are shown in Table 3 and Figure 14 after 7 and 28 days. STS is observed for S3 at 7 and 28 days, with maximum STS of 4.63 MPa and 3.4 MPa, respectively.

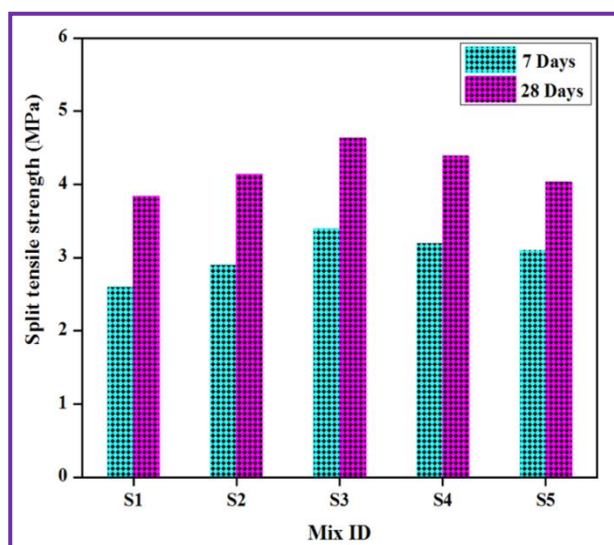


Figure 14. Split tensile strength test

The 7-day STS for mixtures ID-S2 to S5 resulted in an increase in strength of 10.34 %, 23.52 %, 18.75 % and 16.12 % compared to the control samples of mixture ID-S1. The 28-day STS for the mixtures ID -S2 to S5 resulted in a strength increase of 7.24 %, 17.06 %, 12.52 % and 4.71 % compared to the control mixture ID -S1. Overall, the STS of the SCGC improved by 11.44 %. The results of the STS test confirm the behavior of the results of the CS test.

#### 4.3.3. Flexural strength

The FS test for SCGCs with all five correlatives is shown in Table 3 and Figure 15. The maximum FS value for mixture ID -S3 was determined to be 4.28 MPa and 5.85 MPa after 7 and 28 days individually.

The 7-day FS for Mix ID -S2 to S5 developed a strength increase of 6.90 %, 14.95 %, 12.50 % and 4.96 % compared to the control sample of Mix ID -S1. The 28-day FS for Mix ID -S2 to S5 showed an increase in strength of 7.25 %, 16.92 %, 11.95 % and 8.30 % equal to the control sample Mix ID -S1. Overall, the FS of the SCGC improved by 10.59 %.

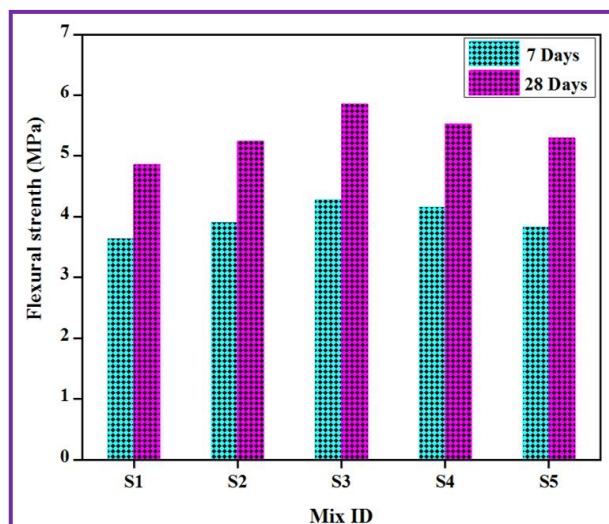


Figure 15. Flexural strength test

#### 4.3.4. Modulus of elasticity

Figure 16 shows in Table 3 and the modulus of elasticity (MOE) for different SCGC mixes (S1 to S5) after 28 days of curing. The results show varying degrees of stiffness improvement compared to the MOE of the S1 control SCGC mix. The MOE of S1 was 26599 MPa, which was used as the base value at 100%.

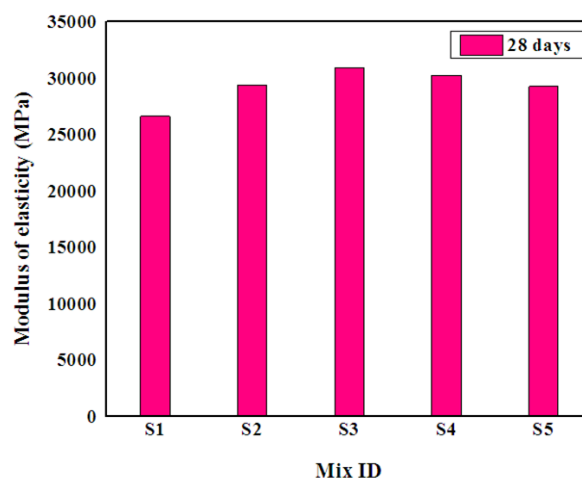


Figure 16. Modulus of elasticity test

The stiffness of mixture of S2, with a slightly higher MOE of 29368, has increased by 10.41% compared to compound S1. Mixture S3 has the highest stiffness with an MOE of 30943 MPa, shows the greatest improvement with an increase of 16.33% compared to the control. Mixture S4 with an MOE of 30249 MPa shows an increase of 13.72%, while mixture S5 with an MOE of 29240 MPa shows an increase of 9.92% compared to S1. These comparisons show that mixture S3 has the largest increase in stiffness compared to the control mixture S1.

## 5. CONCLUSIONS

The following conclusions were drawn based on the research results:

- The fresh properties of the SCGC with A/B ratios of 0.4, 0.45, and 0.5 (Mix ID -S1, S2, and S3) have complied with EFNARC guidelines from the slump flow test. The lowest T50cm slump and time of 696 mm as 4.3 sec were obtained for SCGC with an A/B ratio of 0.5. The V-funnel test also indicated a minimal flow time of 9.8 sec at 0.5 A/B ratios. The height ratio of fresh SCGC was achieved at 0.91 and 0.95 for an A/B ratio of 0.4 and 0.45, respectively. Hence, better workability was attained at an A/B ratio of 0.5 in the SCGC.
- The hardened properties of the SCGC with an A/B ratio of 0.5 was achieved with the highest CS of 38.3 MPa, STS of 4.63 MPa, and FS of 5.85 MPa after 28 days.
- Overall, the A/B ratio of 0.5 was found to be optimal for the FA and GGBS-based SCGC, showing effective improvement in workability as well as increase in strength thereby, resulting in a concrete mix with satisfactory mechanical properties suitable for various construction applications spanning from infrastructure projects to architectural design, repair, and rehabilitation.

## Acknowledgement

The author Vigneshkumar Alagarsamy is grateful to the International Research Centre (IRC), Kalasalingam Academy of Research and Education (KARE) for providing University Research Fellowship (URF) and all the experimental work was carried out at the center for Building Materials, Department of Civil Engineering, KARE.

## 6. REFERENCES

- [1] A.Vigneshkumar, CF.Christy, M.Muthukannan, M.Maheswaran, K.Arunkumar, RK.Devi (2024) Experimental investigations on fresh and mechanical properties of fly ash and ground granulated blast furnace slag self-compacting geopolymer concrete; Materials Today: Proceedings, <https://doi.org/10.1016/j.matpr.2024.01.051>
- [2] A.V, CF.Christy, M.Muthukannan, UJ.Alengaram, M.Maheswaran, N.Johnson Jeyaraj (2024) Study of silicon dioxide nanoparticles on the rheological and mechanical behaviors of self-compacting geopolymer concrete; International Review of Applied Sciences and Engineering, <https://doi.org/10.1556/1848.2024.00794>
- [3] M.Maheswaran, CF.Christy, M.Muthukannan, K.Arunkumar, A.Vigneshkumar (2023) Parametric study on the performance of industrial byproducts based geopolymer concrete blended with rice husk ash & nano silica; Research on Engineering Structures and Materials, <https://doi.org/10.17515/resm2023.809ma0703>
- [4] B.Huang, Y.Zhuge, R.Rameezdeen, K.Xing, G.Huang, Y.Liu (2024) Integrated carbon assessment for sludge-derived concrete; Modelling and a comparative study; Journal of Cleaner Production, 435, 140304. <https://doi.org/10.1016/j.jclepro.2023.140304>
- [5] B.Kanagaraj, N.Anand, E.Lubloy (2024) Utilizing agricultural turmeric bulbs as an alternative to traditional coarse aggregates in geopolymer concrete to explore its engineering properties; Developments in the Built Environment, 17, 100358. <https://doi.org/10.1016/j.dibe.2024.100358>
- [6] A.Singh, SS.Bhadauri, AA.Thakare, A.Kumar, M.Mudgal, S.Chaudhary (2024) Durability assessment of mechanochemically activated geopolymer concrete with a low molarity alkali solution; Case Studies in Construction Materials, 20, 02715. <https://doi.org/10.1016/j.cscm.2023.e02715>
- [7] S.Philip, M.Nidhi, HU.Ahmed (2024) A comparative analysis of tree-based machine learning algorithms for predicting the mechanical properties of fibre-reinforced GGBS geopolymer concrete; Multiscale and Multidisciplinary Modeling, Experiments and Design, 1-29. <https://doi.org/10.1007/s41939-023-00355-6>
- [8] B.Kanagaraj, R.Priyanka, N.Anand, T.Kiran, AD.Andrushia, E.Lubloy (2024) A sustainable solution for mitigating environmental corrosion in the construction sector and its socio-economic concern; Case Studies in Construction Materials, 20, 03089. <https://doi.org/10.1016/j.cscm.2024.e03089>
- [9] M.Thakur, S.Bawa (2022) Self-compacting geopolymer concrete; A review; Materials Today: Proceedings, 59, 1683-1693. <https://doi.org/10.1016/j.matpr.2022.03.400>
- [10] J.Pradhan, S.Panda, SK.Parhi, P.Pradhan, SK.Panigrahi (2024) GGBFS-based self-compacting geopolymer concrete with optimized mix parameters established on fresh, mechanical, and durability characteristics; Journal of Materials in Civil Engineering, 36(2), 04023578. <https://doi.org/10.1061/JMCEE7.MTENG-16669>
- [11] SK.Parhi, S.Dwibedy, SK.Panigrahi (2024) AI-driven critical parameter optimization of sustainable self-compacting geopolymer concrete; Journal of Building Engineering, 86, 108923. <https://doi.org/10.1016/j.jobe.2024.108923>
- [12] YK.Kong, K.Kurumisawa (2023) Fresh properties and characteristic testing methods for alkali-activated materials; A review, Journal of Building Engineering, 75, 106830. <https://doi.org/10.1016/j.jobe.2023.106830>
- [13] MJ.de Hita, M.Criado (2023) Influence of super-plasticizers on the workability and mechanical development of binary and ternary blended cement and alkali-activated cement; Construction and Building Materials, 366, 130272. <https://doi.org/10.1016/j.conbuildmat.2022.130272>
- [14] N.Thatikonda, M.Mallik, SRC.Madduru (2024) Influential studies on microsilica as a potential replacement for fly ash-GGBFS in self-compacting geopolymer concrete: Microstructural insights and performance analysis; Journal of Building Pathology and Rehabilitation, 9(1), 66.

- <https://doi.org/10.1007/s41024-024-00422-6>
- [15] B.Omer, DKl.Jaf, SK.Malla, P.IAbdulrahman, AS. Mohammed, R.Kurda, A. Abdalla (2024) Exploring the potential of soft computing for predicting compressive strength and slump flow diameter in fly ash-modified self-compacting concrete; Archives of Civil and Mechanical Engineering, 24(2), 95. <https://doi.org/10.1007/s43452-024-00910-z>
- [16] T.Yahyaee, HS.Elize (2024) A comprehensive study on mechanical properties, durability, and environmental impact of fiber-reinforced concrete incorporating ground granulated blast furnace slag; Case Studies in Construction Materials, 20, 03190. <https://doi.org/10.1016/j.cscm.2024.e03190>
- [17] P.Azar, G.Samson, C.Patapy, F.Cussigh, L.Frouin, R.Idir, M. Cyr (2024) Durability of sodium carbonate alkali-activated slag concrete assessed by a performance-based approach; Construction and Building Materials, 423, 135873. <https://doi.org/10.1016/j.conbuildmat.2024.135873>
- [18] R.Rawat, D.Pasla (2024) Assessment of mechanical and durability properties of FA-GGBS based lightweight geopolymer concrete; Construction and Building Materials, 426, 135984. <https://doi.org/10.1016/j.conbuildmat.2024.135984>
- [19] N.Hilal, N.Hamah Sor, M.Hadzima-Nyarko, D.Radu, TA.Tawfik (2024) The influence of nanosunflower ash and nanowalnut shell ash on sustainable lightweight self-compacting concrete characteristics; Scientific reports, 14(1), 9450. <https://doi.org/10.1038/s41598-024-60096-5>
- [20] RS.Raj, GP.Arulraj, N.Anand, B.Kanagaraj, E.Lubloy (2024) Nano-bentonite as a sustainable enhancer for alkali activated nano concrete: Assessing mechanical, microstructural, and sustainable properties; Case Studies in Construction Materials, 20, 03213. <https://doi.org/10.1016/j.cscm.2024.e03213>
- [21] HM.Hamada, A.Al-Attar, F.Abed,S. Beddu, AM.Humada, A.Majdi, BS.Thomas (2024) Enhancing sustainability in concrete construction: A comprehensive review of plastic waste as an aggregate material; Sustainable Materials and Technologies, 40, 00877. <https://doi.org/10.1016/j.susmat.2024.e00877>
- [22] M.Hadjadj, M.Guendouz, D.Boukhelkhal (2024) The effect of using seashells as cementitious bio-material and granite industrial waste as fine aggregate on mechanical and durability properties of green flowable sand concrete; Journal of Building Engineering, 87, 108968. <https://doi.org/10.1016/j.jobbe.2024.108968>
- [23] MT.Ghafoor, C. Fujiyama (2024) Effect of Fly Ash Content on Rheological Properties of Self-compacting Geopolymer Mortar; Journal of Advanced Concrete Technology, 22(3), 103-114. <https://doi.org/10.3151/jact.22.103>
- [24] X.Zhao, Z.Xu, W.Tian, JX.Lu, J.Liu, S.Li, Z.Shui (2024) A new scattering-filling process for regulating coarse aggregate and fiber spatial distribution in ultra-high performance concrete; Construction and Building Materials, 416, 135074. <https://doi.org/10.1016/j.conbuildmat.2024.135074>
- [25] X.Su, Z.Ren, P. Li (2024) Review on physical and chemical activation strategies for ultra-high performance concrete (UHPC); Cement and Concrete Composites, 105519. <https://doi.org/10.1016/j.cemconcomp.2024.105519>
- [26] M.Nodehi, F.Aguayo, N.Madey, L.Zhou (2024) A Comparative Review of Polymer, Bacterial-based, and Alkali-Activated (also Geopolymer) Binders: Production, Mechanical, Durability, and Environmental impacts (life cycle assessment (LCA)); Construction and Building Materials, 422, 135816. <https://doi.org/10.1016/j.conbuildmat.2024.135816>
- [27] PD.Nukah, SJ.Abbey, CA.Booth, J.Oti, (2024) Development of low carbon concrete and prospective of geopolymer concrete using lightweight coarse aggregate and cement replacement materials; Construction and Building Materials, 428, 136295. <https://doi.org/10.1016/j.conbuildmat.2024.136295>
- [28] P.Zhang, J.Su, Z.Gao, T.Zhang, P.Zhang (2024) Effect of sand-precursor ratio on mechanical properties and durability of geopolymer mortar with manufactured sand; Reviews on Advanced Materials Science, 63(1), 20230170. <https://doi.org/doi:10.1515/rams-2023-0170>
- [29] X.Ji, Z.Wang, X.Wang, X.Zhao, H.Zhang, T.Zhang (2024) Microstructures and properties of alkali-activated slags with composite activator: Effects of Na<sub>2</sub>O equivalents; Journal of Cleaner Production, 450, 141754. <https://doi.org/10.1016/j.jclepro.2024.141754>
- [30] H.Yong-Jie, H.Cheng-Yong, L.Yun-Ming, MMAB. Abdullah, L.Yeng-Seng, L.Wei-Hao, H.Cheng-Hsuan (2024) Microwave absorption function on a novel one-part binary geopolymer: Influence of frequency, ageing and mix design; Construction and Building Materials, 427, 136264. <https://doi.org/10.1016/j.conbuildmat.2024.136264>
- [31] H.Zhu, X.Wu, Y.Zhang, H. Li (2024) Fast setting and high early strength alkali-activated fly ash synthesized with pre-polymerized suspension combined with ultrafine fly ash at ambient temperature; Case Studies in Construction Materials, 20, e02939. <https://doi.org/10.1016/j.cscm.2024.e02939>
- [32] B.Nikmehr, B.Kafle, R.Al-Ameri (2024) Developing a sustainable self-compacting geopolymer concrete with 100% geopolymer-coated recycled concrete aggregate replacement; Smart and Sustainable Built Environment, 13(2), 395-424.
- [33] C.Clements, L.Tunstall, HG.Bolanos Sosa, A.Hedayat (2024) Improvements in Hydrolytic Stability of Alkali-Activated Mine Tailings via Addition of Sodium Silicate Activator; Polymers, 16(7), 957. <https://doi.org/10.3390/polym16070957>
- [34] G. Gaurav, SC.Kandpal, D.Mishra, N.Kotoky (2024) A comprehensive review on fly ash-based geopolymer: a pathway for sustainable future; Journal of Sustainable Cement-Based Materials, 13(1), 100-144. <https://doi.org/10.1080/21650373.2023.2258122>
- [35] R.Priyanga, A.Muthadhi (2024) Effect of Fiber Meshes on Compression Performance of Textile Reinforced Concrete Based on Response Surface Method; Iranian Journal of Science and Technology, Transactions of Civil Engineering, 1-19. <https://doi.org/10.1007/s40996-024-01423-8>

- [36] J.Zhang, S.Wu, Y.Li, Z.Song, X.Dong, Y.Zhang, Y, B.Xiao (2024) Experimental study on cement-based materials for grouting/replacement of broken rock mass in coal mine; Construction and Building Materials, 425, 135979. <https://doi.org/10.1016/j.conbuildmat.2024.135979>
- [37] K.BA, N.VK Data Visualization and Interpretation for Hardened Properties of Geopolymer Concrete Using Machine Learning and Python; Available at SSRN 4688822.
- [38] X.Tian, J.Shuai, J.Wu, Q.Zhong, Z.Liu, Z.Jin (2024) Understanding the influence of compressive strength, microstructure, and mechanism for metakaolin-based geopolymer under varying rest periods in the curing process; Construction and Building Materials, 427, 136239. <https://doi.org/10.1016/j.conbuildmat.2024.136239>
- [39] M.Nasir, AH.Mahmood, AA.Bahraq (2024) History, recent progress, and future challenges of alkali-activated binders—An overview; Construction and Building Materials, 426, 136141. <https://doi.org/10.1016/j.conbuildmat.2024.136141>
- [40] J.Oti, BO.Adeleke, PR.Mudiysanlagel, J.Kinuthia (2024) A Comprehensive Performance Evaluation of GGBS-Based Geopolymer Concrete Activated by a Rice Husk Ash-Synthesised Sodium Silicate Solution and Sodium Hydroxide; Recycling, 9(2), 23. <https://doi.org/10.3390/recycling9020023>
- [41] M.Umer, J.Ahmad, H.Mukhtar (2024) Innovative valorization of biomass waste-derived sodium silicate for geopolymer concrete synthesis: Sustainability assessment and circular economy potential; Journal of Cleaner Production, 452, 142181. <https://doi.org/10.1016/j.jclepro.2024.142181>
- [42] O.Zaid, MH.El Ouni (2024) Advancements in 3D printing of cementitious materials: A review of mineral additives, properties, and systematic developments; Construction and Building Materials, 427, 136254. <https://doi.org/10.1016/j.conbuildmat.2024.136254>
- [43] N.Johnson Jeyaraj, V.Sankararajan (2024) Study on the characterization of fly ash and physicochemical properties of soil, water for the potential sustainable agriculture use—A farmer's perspectives; International Review of Applied Sciences and Engineering, 15(1), 95-106. <https://doi.org/10.1556/1848.2023.00661>
- [44] Z.Pan, M.Tan, G.Zheng, L.Wei, Z.Tao, Y. Hao (2024) Effect of silica fume type on rheology and compressive strength of geopolymer mortar; Construction and Building Materials, 430, 136488. <https://doi.org/10.1016/j.conbuildmat.2024.136488>
- [45] I.Faridmehr, ML.Nehdi, GF.Huseien, MH.Baghban, ARM.Sam, HA.Algaifi (2021) Experimental and informational modeling study of sustainable self-compacting geopolymer concrete; Sustainability, 13(13), 7444. <https://doi.org/10.3390/su13137444>
- [46] I.Standard (1999) Indian standard Splitting tensile strength of concrete-method of test (first revision), IS, 5816, 1-14.

## IZVOD

### UTICAJ ALKALNIH VEZIVA NA OBRADLJIVOST I ČVRSTOĆU SAMOSKUPLJAJUĆEG GEOPOLIMER BETONA

*Samozbijajući geopolimer beton (SCGC) je obećavajuća alternativa tradicionalnom betonu zbog svojih ekoloških prednosti. U SCGC, alkalna veziva kao što su natrijum hidroksid (NaOH) i natrijum silikat ( $\text{Na}_2\text{SiO}_3$ ) imaju potencijal da utiču na obradivost i snagu. Konkretno, odnos alkalnih veziva direktno utiče na ukupne performanse SCGC. U ovom istraživanju pet SCGC se meša sa različitim odnosima alkalnog veziva između 0,40 i 0,60 u 50% letećeg pepela (FA) i 50% mlevene granulirane šljake visoke peći (GGBS), u koncentraciji 14 M NaOH, superplastifikator (9 kg/m<sup>3</sup>). I dodatne vode (54 kg/m<sup>3</sup>) ispitan je uticaj odnosa alkalnog veziva na obradivost i svojstva mehaničke čvrstoće. Rezultati studije su pokazali da su sveža svojstva SCGC-a sa A/B odnosima od 0,4, 0,45 i 0,5 u skladu sa smernicama EFNARC-a iz testa sleganja, a najniži dobijeni pad T50cm bio je 696 mm. Postignut je najveći CS od 38,3 MPa, STS od 4,63 MPa i FS od 5,85 MPa, što ukazuje na bolje mehaničke performanse SCGC mešavine sa odnosom A/B od 0,5. Zbog toga su odnosi alkalnog veziva od 0,5 optimizovani na 14 M NaOH na reološkim svojstvima i svojstvima čvrstoće.*

**Ključne reči:** leteći pepeo, GGBS, NaOH,  $\text{Na}_2\text{SiO}_3$ , odnos alkalnog veziva, reološka i mehanička svojstva.

*Naučni rad*

*Rad primljen: 18.07.2024.*

*Rad korigovan: 28.09.2024.*

*Rad prihvaćen: 02.10.2024.*

Vigneshkumar Alagarsamy:  
Clementz Edwardraj Freeda Christy:  
Muthukannan Muthiah:  
Ubagaram Johnson Alengaram:

<https://orcid.org/0009 0003 4755 8669>  
<https://orcid.org/0000 0002 6929 310X>  
<https://orcid.org/0000 0003 1912 3513>  
<https://orcid.org/0000 0001 9358 2975>